Letters

Conditional Sixth-Harmonic Injection to Improve the Linear Modulation Range of Three-Phase Voltage-Source Converters

Anubrata Das, *Member, IEEE*, Fred Wang, *Fellow, IEEE*, and Yaosuo Xue, *Senior Member, IEEE*

***Abstract*—Overmoduation techniques are used to improve dc bus voltage utilization for three-phase voltage-source converters (VSCs), resulting in significant reduction in fundamental voltage gain. Conventional pulsewidth modulation (PWM) techniques for three-phase VSCs cannot enhance the linear range of dc bus utilization by more than 15.5%. In this letter, a conditional sixth-harmonic injection technique is introduced, which can theoretically improve the linear modulation range by up to 19.2% for three-phase ac systems without additional hardware components. Experimental validation of the proposed scheme is presented, with its performance compared against the conventional third-harmonic PWM technique.**

***Index Terms*—Conditional harmonic injection, electromagnetic interference (EMI), linear modulation range, overmodulation (OVM), pulsewidth modulation (PWM), three-phase drive, total harmonic distortion (THD).**

I. Introduction

IMPROVING dc bus voltage utilization is desirable for ac voltage-source converters. This leads to the development of several overmodulation (OVM) techniques both for multiphase [1], [2], [3] and three-phase converters [4], [5], [6]. These techniques offer fault-tolerant operation to some extent during dc bus undervoltage events. While OVM techniques enhance dc bus voltage utilization, they come with drawbacks, such as a significant decrease in fundamental voltage gain, uneven triggering of gate driver circuits in the OVM zone, instability in closed-loop control, and potential false tripping of drive protection circuits. To address these issues, several pulsewidth modulation (PWM) techniques have been proposed, particularly for multilevel inverters, aiming to improve the linear modulation range [7], [8]. While these techniques are useful, they are primarily developed for multiphase or multilevel ac drives, where leveraging the full dc-link voltage with a lower modulation index is feasible compared to three-phase ac drives [9]. Consequently, these techniques cannot be readily adapted for three-phase ac drive applications. Moreover, most of these techniques rely on programmed pulsed modulation methods, which pose a drawback in terms of computational time compared with carrier-based PWM techniques. This computational time may affect the minimum dead time requirement of converter switches, particularly in low-cost applications with controllers of limited computational capacity.

To enhance the linear modulation range particularly for three-phase systems, zero-sequence-harmonic-injection-based PWM techniques, such as third-harmonic-injection-based PWM, space-vector-modulation-based pulsewidth modulation (SVPWM), and discontinuous PWM, are proposed. While these techniques have proved to be effective and easy to implement, they cannot enhance dc bus utilization by more than 15.5%.

Addressing these research gaps, this letter proposes a carrier-based PWM strategy for three-phase ac drives to improve the linear modulation range more than 15.5% with the conventional zero-sequence-harmonic-injection-based PWM techniques. No additional hardware is required to realize the proposed PWM technique.

II. Proposed Technique

A. Basis of Harmonic Injection

In the case of third-harmonic-injection-based PWM, the fundamental signal can be increased by 15.5%. The magnitude of the injected third-harmonic signal is found maximizing the following equation:

$$y = k_1 \sin(\omega t) + k_3 \sin(3\omega t) \tag{1}$$

where k_1 and k_3 are coefficients of fundamental and third-harmonic signals, respectively. For the third-harmonic-injection-based PWM technique, the optimal value of k_3 is one-sixth of the fundamental signal. If a higher order harmonic component (ninth harmonic) is injected along with third-harmonic signal, then the resultant modulation signal approaches the SVPWM technique [10]. Although SVPWM has superior performance characteristics than other PWM techniques, it cannot improve the fundamental signal magnitude by more than 15.5%. The proposed control method can improve the linear operating

Manuscript received 1 June 2024; revised 8 July 2024; accepted 8 August 2024. Date of publication 26 August 2024; date of current version 7 October 2024. This work was supported by the U.S. Department of Energy, Office of Electricity, Advanced Grid Modeling Program, under Contract DE-AC05-00OR22725. *(Corresponding author: Anubrata Das.)*

Anubrata Das and Fred Wang are with the Department of Electrical Engineering and Computer Science, University of Tennessee, Knoxville, TN 37996 USA (e-mail: anubrata0103@gmail.com; f.wang@ieee.org).

Yaosuo Xue is with Oak Ridge National Laboratory, Oak Ridge, TN 37830 USA (e-mail: yx@ieee.org).

Color versions of one or more figures in this article are available at https://doi.org/10.1109/TPEL.2024.3445870.

Digital Object Identifier 10.1109/TPEL.2024.3445870

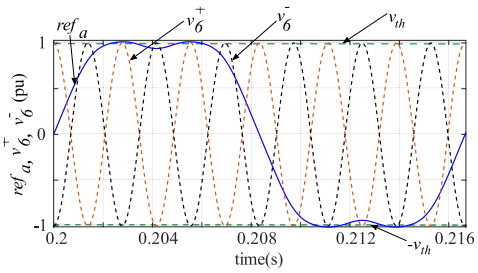

Fig. 1. ref_a (blue), $v^+{}_6$ (brown dashed), $v^-{}_6$ (black dashed), and $\pm v_{\text{th}}$ (green dashed).

range more than 15.5%. The proposed technique consists of three control modules as follows.

B. Generation of Reference Signals

The reference signals of all the three phases are generated separately. Reference signals are the combination of fundamental (v_1), third-harmonic (v_3), and ninth-harmonic (v_9) frequency signals. The following equation depicts the reference signal for phase a (ref_a):

$$\text{ref}_a = k_1\, v_{1a} + k_3 v_3 + k_9 v_9 \tag{2}$$

where v_1, v_3, and v_9 are the fundamental, third-harmonic, and ninth-harmonic signals of magnitude 1.0 p.u., respectively, and subscript a denotes phase a.

1) Selection of k_3 and k_9: k_3 and k_9 can be selected by solving the transcendental equation in (2). However, this is computationally exhaustive. Therefore, these coefficients are optimally selected by varying k_1 from 1.15 to 1.27 p.u. (spanning from the onset of OVM for conventional modulation techniques to six-step operation). k_3 and k_9 are swept from –1 to +1 with a step size of 0.001 for each value of k_1. The selection of optimal values for k_3 and k_9 adheres to two criteria: 1) the positive (or negative) peak magnitude of the reference signal in (2) should not exceed $\sqrt{3}k_1/2$ (or $-\sqrt{3}k_1/2$), and 2) the positive peaks of the reference signal should occur at $(6n+1)\times 60°$ and $(3n+1)\times 120°$. This is because, without the conditional sixth-harmonic injection, the modulation signal should have similar characteristics as SVPWM or third-harmonic-injection-based PWM techniques. Following these criteria, the values of k_3 and k_9 are determined to be $k_1/5.2$ and –0.01, respectively.

C. Generation of the Sixth-Harmonic Signal

If the k_1 value exceeds 1.15 p.u., it would cause the peak of the ref_a signal to surpass ±1.0 p.u., as illustrated in Fig. 1. To limit the magnitude of ref_a to 1.0 p.u., a sixth-harmonic signal (v_6) is conditionally injected. Notably, the positive peak of ref_a occurs every $(6n+1)\times 60°$ and $(3n+1)\times 120°$ (n is a positive integer), while the positive peak of v_6 aligns with every $(6n+1)\times 60°+15°$ and $(3n+1)\times 120°+15°$. To synchronize the peaks of both the signals, v_6 is phase advanced by 15° and denoted as $v^+{}_6$. Correspondingly, $v^-{}_6$ is generated for the negative half-cycle, which is essentially the 180° phase-shifted version of $v^+{}_6$, achieved by multiplying –1 with $v^+{}_6$. Fig. 1 displays $v^+{}_6$ (brown dashed) and $v^-{}_6$ (black dashed) signals. As discussed, the peak of $v^+{}_6$ aligns with the positive peaks of the ref_a signal, while $v^-{}_6$ aligns with the negative peaks of the ref_a signal.

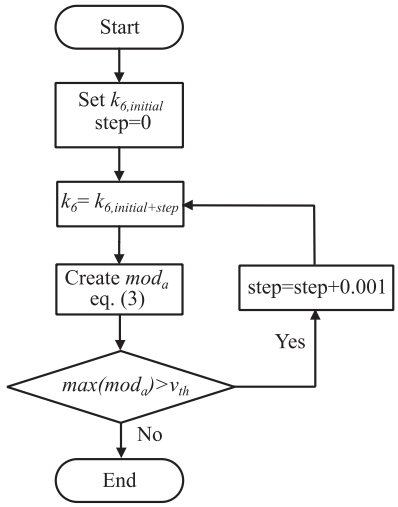

Fig. 2. Flowchart for k_6 selection.

D. Generation of the Modulation Signal

In the proposed technique, $v^+{}_6$ and $v^-{}_6$ signals are not always injected. Whenever the ref_a signal crosses v_{th} in the positive half-cycle, the $v^+{}_6$ signal is multiplied with a gain k_6 and subtracted from ref_a. Similarly, when ref_a crosses $-v_{\text{th}}$ in the negative half-cycle, the $v^-{}_6$ signal is multiplied by k_6 and subtracted from ref_a. Therefore, the modulation signal for phase a (mod_a) is expressed as

$$\begin{aligned}\text{mod}_a &= \text{ref}_a - k_6 v_6^+ \rightarrow \text{test}_a \geq\ v_{\text{th}}\\ &= \text{ref}_a\ - k_6 v_6^- \rightarrow \text{test}_a \leq -v_{\text{th}}\\ &= \text{ref}_a \rightarrow \text{otherwise}.\end{aligned} \tag{3}$$

This exercise is performed for all the other phases since the reference signal for phases a–c crosses $\pm v_{\text{th}}$ at different instants. In general, v_{th} can be set as ±1.0 p.u.

1) Selection of k_6: The value of k_6 should be such that the $v^+{}_6$ and $v^-{}_6$ signals are able to reduce the peak of the reference signal below $\pm v_{\text{th}}$. In the proposed algorithm, k_6 is found in an iterative manner, as shown in Fig. 2. The difference between the reference signal and v_{th} is calculated, which is k_1 ($\sqrt{3}/2-1$). The inverse of this difference is set to be the starting point of k_6. $v^+{}_6$ and $v^-{}_6$ are generated using this value of k_6, and the modulation signal is generated using (2). If the peak of the modulating signal is still found to be beyond $\pm v_{\text{th}}$, the k_6 gain is increased with a step of 0.001 until the peak of modulating signal comes below v_{th}.

2) Limit of k_1: k_1 is the coefficient of the fundamental signal. The magnitude of k_1 determines the intersection points of the reference signal and v_{th}. Higher value of k_1 increases the span over which the reference signal remains greater than or lesser

than ± 1 (without injecting $v^+{}_6$ and $v^-{}_6$). For the proposed algorithm to work desirably, the reference in (1) must intersect $\pm v_{\text{th}}$ four times in every half-cycle. Otherwise, the injected $k_6 v^+{}_6$ (or $k_6\, v^-{}_6$) would increase the peak of the resultant signal instead of limiting it to ± 1 p.u. From this condition, the maximum value of k_1 is found using the following equations:

$$k_1 \sin(\theta) + k_3 \sin(3\theta) + k_9 \sin(9\theta) = 1 \quad \text{while} \quad k_6 \sin 6(\theta + 15^\circ) \geq 0 \tag{4}$$

or

$$k_1 \sin(\theta) + k_3 \sin(3\theta) + k_9 \sin(9\theta) = -1 \quad \text{while} \quad k_6 \sin 6(\theta + 15^\circ) \leq 0. \tag{5}$$

In (4), the solution of θ must be real in $[0, m\pi/2]$ interval (m is an odd integer). Solving (4) with this condition, the maximum value of k_1 *is* found to be 1.192 p.u. In a similar way, (5) can be used to find the maximum value of k_1.

III. Effect in System Performance

In this section, how the proposed techniques affect the system performance is investigated.

A. Total Harmonic Distortion

The conditionally injected sixth-harmonic voltage is not strictly coplanar and would not be canceled in the line voltage. The non-tri-planar harmonics are found by performing Fourier analysis on the conditionally injected sixth-harmonic voltage. It is worth noting that the conditional sixth-harmonic voltage has odd (on fundamental axis time scale) and quarter wave symmetry. The Fourier coefficient is found as

$$\begin{aligned} b_n &= \frac{4}{\pi} \int_{\alpha_1}^{\alpha_2} k_6 \sin\left(6\omega t - \frac{\pi}{2}\right) \sin(n\omega t)\, d(\omega t) \\ &= \frac{2k_6}{\pi} \left[\frac{1}{6-n} \{\cos(6-n)\alpha_2 - \cos(6-n)\alpha_1\}\right] \\ &\quad + \frac{2k_6}{\pi} \left[\frac{1}{6+n} \{\cos(6+n)\alpha_2 - \cos(6+n)\alpha_1\}\right] \end{aligned} \tag{6}$$

where α_1 and α_2 are the intersection points of reference signal with the v_{th} signals. It is inferred from (6) that the magnitude of b_n increases with the increasing difference in the values of α_2 and α_1. Hence, the harmonics in the line voltage increase with the increasing magnitude of k_1. This is further validated in Section IV.

B. Common-Mode Voltage

To assess the performance of the proposed technique in terms of the common-mode (CM) voltage generation, the CM volt–second estimation method [11] is adapted, given as

$$|V_{\text{cm}}| = \frac{T_0 |V_{\text{dc}}| + (T_s - T_0) \left|\frac{V_{\text{dc}}}{3}\right|}{T_s} \times \frac{C_S}{C_s + 2C_y} \tag{7}$$

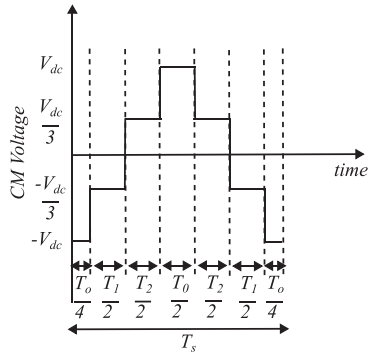

Fig. 3. CM voltage in the time domain.

where T_s and T_0 are the switching period and the duration of zero-voltage vector, V_{dc} is half the dc-link voltage, and C_s and C_y are the stray capacitance between the load terminal and ground and CM capacitance, respectively, as shown in Fig. 3. From (7), the CM voltage is a function T_0 and V_{dc}. For a given modulation index (in this case k_1), the duration of T_0 in case of third-harmonic PWM or SVPWM and the proposed PWM technique are same. Therefore, the CM electromagnetic interference (EMI) performance of these techniques would be similar. This is validated in Section IV by comparing the proposed technique with third-harmonic injection PWM.

C. Losses

The PWM schemes differ from each other only because of differences in the zero-voltage vector placement. For the three-wire system, $i_a + i_b + i_c = 0$ makes the difference in the conduction loss among different PWM schemes negligible. The expression for the forward conduction loss with the majority carrier device, such as MOSFET, for third-harmonic injection PWM and the proposed technique is given as follows:

$$P^{\text{third}}_{\text{fwd,cond}} = R^{\text{fwd}}_{\text{on}}\, I^2_M \left[\frac{1}{8} + \frac{k_1}{3\pi}\cos\phi - \frac{k_3}{15\pi}\cos 3\phi\right] \tag{8}$$

$$P^{\text{proposed}}_{\text{fwd,third}} = P^{\text{third}}_{\text{fwd,cond}} - R^{\text{fwd}}_{\text{on}} I^2_M \times \frac{k_9}{693\pi} \cos 9\phi \tag{9}$$

where ϕ is the power factor angle, and $P^{\text{third}}_{\text{fwd,cond}}$ and $P^{\text{proposed}}_{\text{fwd,third}}$ are the forward conduction loss for third-harmonic injection PWM and the proposed PWM technique, respectively. From (9), it can be inferred that the term containing k_9 is practically negligible for any $k_9 < 1.0$. Thus, the forward conduction loss with the proposed PWM technique is practically same as third-harmonic injection PWM. A similar discussion can be extended for reverse conduction loss.

Switching loss depends on switching frequency, operating conditions, and device characteristics. Hence, for the same operating conditions, the switching loss would also be same for these two techniques for a given type of device and switching frequency.

TABLE I
PARAMETERS OF THE EXPERIMENTAL SETUP

Parameter	Value
AC drive	f_s=10 kHz, L_f=0.5 mH, R_f=50mΩ, C_f=150 μF 380 V, 140 A 3-Ph output
Applied DC Voltage	V_{dc}=100 V
Load	R_{load}=10 Ω, L_{load}=0.7 mH

D. Dependence on Switching Frequency

The ratio of the switching frequency to the fundamental frequency is not a prohibitive factor for the proposed scheme. In the proposed scheme, conditional sixth- and ninth-harmonic signals are added with the reference signal in a feedforward manner. Therefore, these harmonics appear directly at the inverter terminal (before the filter) and remain unaffected by the filter attenuation characteristics. Therefore, the proposed scheme is equally effective as other zero-sequence-injection-based PWM techniques even for low switching frequency applications.

E. Enhancement of the Linear Modulation Range

To quantify the linear modulation range, the approach in [10] is used in this work, given as

$$G = k_1 / k_1^* \tag{10}$$

where $k^*{}_1$ and k_1 are the peak magnitude (in p.u.) of fundamental voltage without saturation and with saturation respectively, and G is the linear modulation gain. From (10), the magnitude of G is 1 till the point k_1 is equal to $k_1{}^*$. Therefore, beyond the linear modulation range, G value keeps on decreasing, thus resulting in the reduced utilization of dc bus voltage as compared to linear modulation range. The expression of G for different modulation schemes is derived in [10]. Since the proposed technique can maintain the magnitude of the modulation signals (mod_a, mod_b, and mod_c) by ± 1.0 p.u. for $k^*{}_1$ value 1.19, with the proposed technique, the value of G remains 1.0 till $k^*{}_1 = 1.19$ p.u. This is validated in Section IV.

It is worth mentioning that the concept of gain G is not valid for square wave modulation. In this case, the modulation signal is saturated to 1.0 or –1.0 p.u. value in the positive and negative half-cycles, respectively. Therefore, there is no linear modulation range in case of square wave or six-step modulation.

IV. RESULTS AND DISCUSSIONS

The proposed technique is validated in an experimental prototype. The experimental setup consists of a two-level three-phase three-wire ac drive (Vacon make) and three-phase *RL* load. Texas Instruments makes TMS320F28335 digital signal processor used to control the ac drive. The experimental parameters are tabulated in Table I. The experimental line voltages and current waveforms are shown in Fig. 4 for $k_1 = 1.17$.

A. Total Harmonic Distortion Performance

Due to conditional sixth-harmonic voltage injection, the line voltages contain small harmonics, as illustrated in Fig. 5. The harmonic components and total harmonic distortion (THD) are

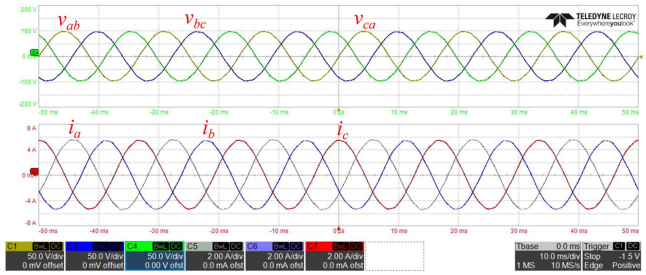

Fig. 4. Experimental results for $k_1 = 1.19$. Top: line voltages (*Y*-axis: 50 V/div and *X*-axis: 10 ms/div). Bottom: line currents (*Y*-axis: 2 A/div and *X*-axis: 10 ms/div).

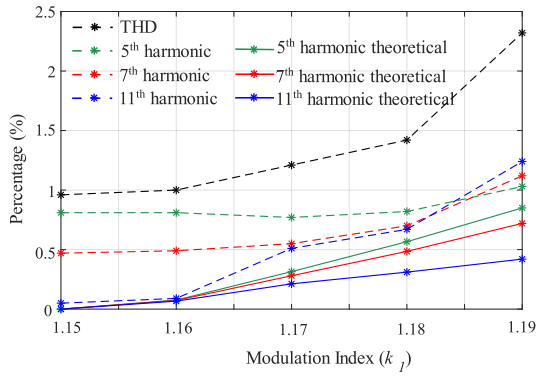

Fig. 5. Harmonic performance with increasing fundamental signal magnitude.

calculated in MATLAB using data points obtained from experiments conducted with a Lecroy MDA 810 oscilloscope. From Fig. 5, it is observed that for a k_1 value of 1.15, which marks the onset of the OVM region for conventional PWM techniques, the line voltage THD is 0.96%. The THD value increases with higher values of k_1 because larger magnitudes of k_6 are required to limit the modulation signal within the $\pm v_{\text{th}}$ limit, which is in close agreement with the theoretical results. The difference in the theoretical and experimental harmonic distortion can be attributed to nonlinearities introduced by dead time or device turn ON/OFF dynamics. It is noted from experimental results that even for a k_1 value of 1.19 (the theoretical maximum value of k_1 being 1.192), the line voltage THD remains below 2.5%. Such minor harmonic contents can be easily mitigated with a small passive filter at the load input terminal.

B. Linear Modulation Region Improvement Performance

To demonstrate the efficacy of the proposed technique in terms of improving the linear modulation range, the fundamental voltage magnitude of line–line voltage for different values of the fundamental signal is measured from experiments and compared with third-harmonic PWM. In Fig. 6, the fundamental voltage magnitude with these two modulation schemes is shown.

As can be seen from Fig. 6, the increase in the fundamental voltage magnitude with the proposed technique is almost linear for k_1 greater than 1.15, while for third-harmonic PWM, it is not linear. This result is in line with the theoretical gain G discussion in the previous section.

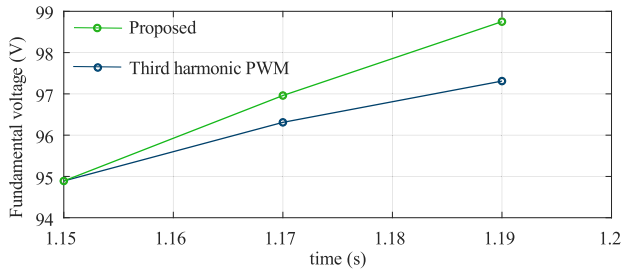

Fig. 6. Fundamental component of line–line voltage obtained from experiments. Traces: proposed technique (green) and third-harmonic PWM (blue).

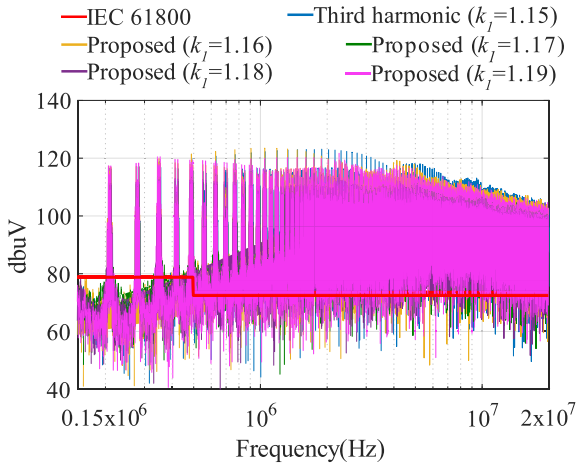

Fig. 7. CM EMI noise for different values of k_1.

C. CM EMI Performance

The EMI performance of the proposed technique is assessed through simulation. The study considers a three-phase two-level inverter with a nominal rating of 3.8 kW and 220-V (line-to-line) voltage. The inverter operates at a switching frequency of 70 kHz. CM noise is measured using a line impedance stabilization network at the terminals of the inverter. A three-phase motor model, with both the high and low frequencies, serves as the load for the inverter. Fig. 7 illustrates the bare CM noise with the proposed technique for various values of k_1. In addition, the CM noise with conventional third-harmonic PWM at $k_1 = 1.15$ is plotted on the same graph to facilitate a comparison of EMI performance. The results shown in Fig. 7 are in close agreement with the discussion and derivation in Section III. This emphasizes the fact that the proposed technique does not require any special design considerations for a CM EMI filter.

V. Conclusion

A conditional sixth-harmonic injection technique is introduced to enhance the linear modulation range of three-phase converters. The proposed technique theoretically extends the linear modulation range by 19.2%. Experimental and simulation results validate the effectiveness of the proposed scheme. EMI performance analysis reveals that the proposed technique is comparable to conventional third-harmonic PWM. In addition, it is observed that the harmonic content of the line voltage increases with higher values of k_1 (for $k_1 > 1.15$), which can be mitigated using conventional harmonic suppression techniques at the load terminal. Thus, the proposed technique proves to be advantageous, particularly during dc undervoltage events or sudden torque requirements by the ac motor.

Notice of Copyright

References

[1] M. J. Durán, J. Prieto, and F. Barrero, "Space vector PWM with reduced common-mode voltage for five-phase induction motor drives operating in overmodulation zone," *IEEE Trans. Power Electron.*, vol. 28, no. 8, pp. 4030–4040, Aug. 2013, doi: 10.1109/TPEL.2012.2229394.

[2] S. Paul and K. Basu, "A three-phase inverter based overmodulation strategy of asymmetrical six-phase induction machine," *IEEE Trans. Power Electron.*, vol. 36, no. 5, pp. 5802–5817, May 2021, doi: 10.1109/TPEL.2020.3026816.

[3] G. Yang et al., "Overmodulation strategy for seven-phase induction motors with optimum harmonic voltage injection based on sequential optimization scheme," *IEEE Trans. Power Electron.*, vol. 36, no. 12, pp. 14039–14050, Dec. 2021, doi: 10.1109/TPEL.2021.3083974.

[4] S. Bolognani and M. Zigliotto, "Novel digital continuous control of SVM inverters in the overmodulation range," *IEEE Trans. Ind. Appl.*, vol. 33, no. 2, pp. 525–530, Mar./Apr. 1997, doi: 10.1109/28.568019.

[5] J. Holtz, W. Lotzkat, and A. Khambadkone, "On continuous control of PWM inverters in the overmodulation range including the six-step mode," in *Proc. Int. Conf. Ind. Electron., Control, Instrum., Autom.*, 1992, vol. 1, pp. 307–312, doi: 10.1109/IECON.1992.254615.

[6] Z. Li, Y. Guo, K. Huang, and X. Zhang, "Synchronized SVPWM algorithm based on superposition principle for the overmodulation region at low switching frequency," in *Proc. 19th Int. Conf. Elect. Mach. Syst.*, 2016, pp. 1–6.

[7] A. R. S, S. Pramanick, R. S. Kaarthik, K. Gopakumar, and F. Blaabjerg, "Extending the linear modulation range to the full base speed using a single DC-link multilevel inverter with capacitor-fed H-bridges for IM drives," *IEEE Trans. Power Electron.*, vol. 32, no. 7, pp. 5450–5458, Jul. 2017, doi: 10.1109/TPEL.2016.2610458.

[8] T. T. Davis and A. Dey, "Investigation on extending the DC bus utilization of a single-source five-level inverter with single capacitor-fed H-bridge per phase," *IEEE Trans. Power Electron.*, vol. 34, no. 3, pp. 2914–2922, Mar. 2019, doi: 10.1109/TPEL.2018.2844323.

[9] L. Vancini, M. Mengoni, G. Rizzoli, G. Sala, L. Zarri, and A. Tani, "Carrier-based PWM overmodulation strategies for five-phase inverters," *IEEE Trans. Power Electron.*, vol. 36, no. 6, pp. 6988–6999, Jun. 2021, doi: 10.1109/TPEL.2020.3034170.

[10] A. M. Hava, "Carrier-based PWM-VSI drives in the overmodulation region," Ph.D. dissertation, Dept. Elect. Comput. Eng., Univ. Wisconsin Madison, Madison, WI, USA, 1998.

[11] F. Luo et al., "Analysis of CM volt-second influence on CM inductor saturation and design for input EMI filters in three-phase DC-fed motor drive systems," *IEEE Trans. Power Electron.*, vol. 25, no. 7, pp. 1905–1914, Jul. 2010, doi: 10.1109/TPEL.2010.2043541.